LBNL-1003927

ERNEST ORLANDO LAWRENCE
BERKELEY NATIONAL LABORATORY

Integrated control of dynamic facades and distributed energy resources for energy cost minimization in commercial buildings

Eleanor S. Lee, Christoph Gehbauer, Brian E. Coffey, Andrew McNeil, Michael Stadler, Chris Marnay

Energy Technologies Area
November 2015

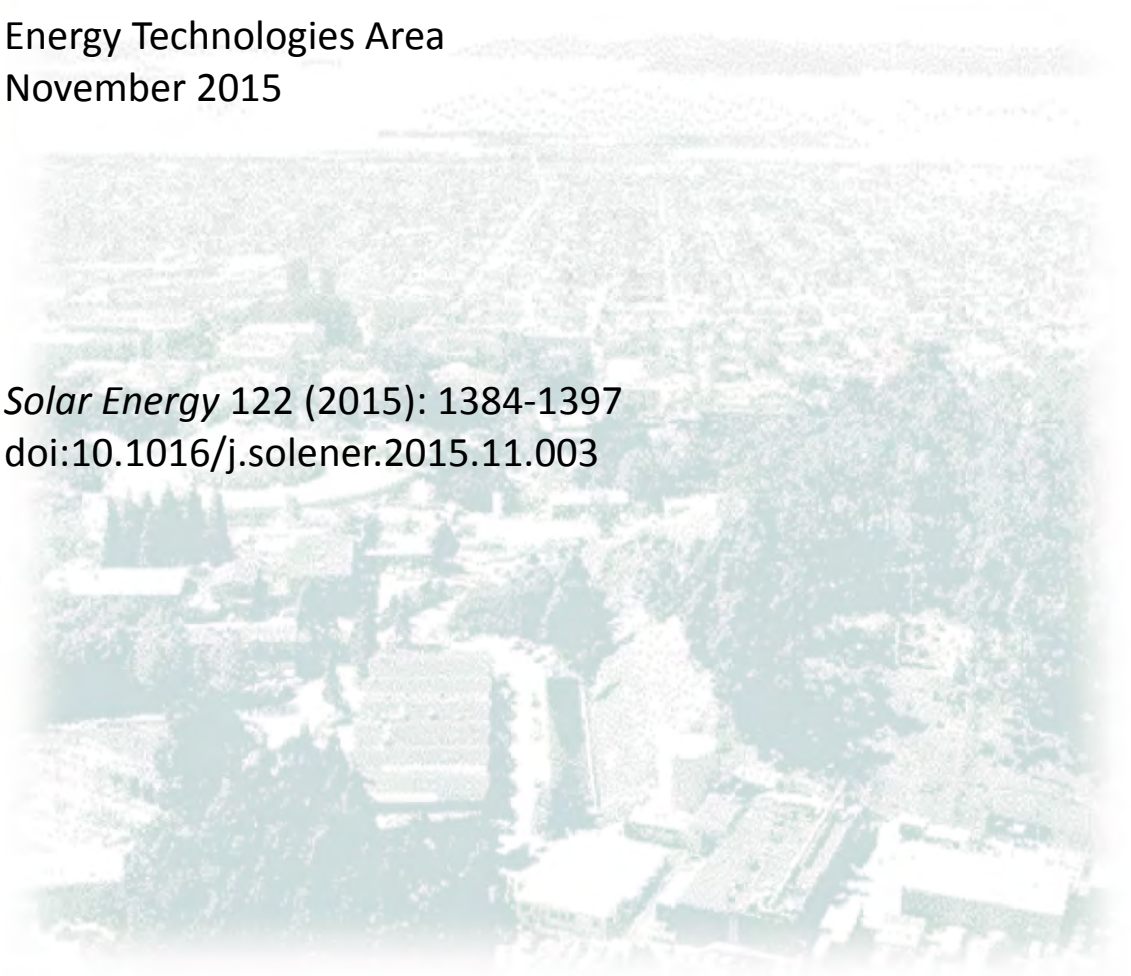

Solar Energy 122 (2015): 1384-1397
doi:10.1016/j.solener.2015.11.003

Disclaimer

Acknowledgments

We would like to acknowledge the contributions of our LBNL colleagues: Michael Wetter, Dennis DiBartolomeo, Darryl Dickerhoff, Wei Feng, and Anothai Thanachareonkit. We would also like to thank Sage Electrochromics and Saint-Gobain North America for their in-kind support for the field test.

Implementation and testing of the loads-to-DERCAM control module was conducted as part of Christoph Gehbauer's master's thesis under the supervision of Professor Hubert Fechner at the Renewable Urban Energy Systems Department of the University of Applied Sciences Technikum, Wien, and financially supported by the Austrian Marshall Plan Foundation.

This work was supported by the Assistant Secretary for Energy Efficiency and Renewable Energy, Office of Building Technology, State and Community Programs, Office of Building Research and Standards of the United States Department of Energy under Contract No. DE-AC02-05CH11231 and by the California Energy Commission through its Public Interest Energy Research (PIER) Program on behalf of the citizens of California.

Solar Energy 122 (2015): 1384-1397

Integrated control of dynamic facades and distributed energy resources for energy cost minimization in commercial buildings

Eleanor S. Lee[a1], Christoph Gehbauer[a], Brian E. Coffey[a], Andrew McNeil[a], Michael Stadler[b], Chris Marnay[c]

Building Technologies and Urban Systems Division [a], Energy Storage and Distributed Resources Division [b], and Energy Analysis and Environmental Impacts Division [c], Energy Technologies Area, Lawrence Berkeley National Laboratory, 1 Cyclotron Road, Berkeley, California, USA

Abstract

Controllable window, shading, and daylighting technologies provide an interesting opportunity to manage end use demands on distributed energy resources (DER) in ways that both complements the peak output profile of solar photovoltaic (PV) electricity generation and counteracts the peak demands on the utility grid produced by daytime commercial activities. The objective of this study is to explore whether dynamic facade technologies can play an enabling role in supporting a desired level of electricity service at either minimum operating cost or minimum carbon footprint through optimized integrated control with distributed energy resources. A proof-of-concept control system was developed by approximating non-linearities as piecewise-linear and determining the control state of both the demand and supply side components through global optimization. Annual simulations of a south-facing office zone with switchable electrochromic windows, solar photovoltaic electricity generation, and battery storage indicated that with optimized integrated demand-supply side controls, the utility grid load profile could be lowered to nearly zero demand (5 W/m^2) during the daytime when energy costs are highest. A full-scale outdoor field test in Berkeley, California verified this performance, demonstrating that during a week of sunny winter weather, electricity bills could be reduced by 63% compared to heuristic control of electrochromic windows without the photovoltaics and electrical storage. In both the simulated and measured cases, the photovoltaic system was sized to meet the peak perimeter zone load and the electrical storage was sized to be fully discharged by the end of the peak day. Technical and market challenges for achieving reliable optimal control for widespread applications are discussed.

Keywords: Distributed energy resources; Demand side management; Zero net energy buildings; Dynamic windows; Control optimization

1. Introduction

Distributed energy resources (DER) promise economic, environmental and utility system benefits. Small-scale, distributed electricity generation acts as a hedge against electricity price fluctuation and addresses

.

[1] Corresponding author at: Lawrence Berkeley National Laboratory, Mailstop 90-3111, 1 Cyclotron Road, Berkeley, California 94720 United States of America, Tel.: 510-486-4997. E-mail address: eslee@lbl.gov, (E.S. Lee).

power quality and reliability concerns caused by failures in the utility network, large voltage drops due to switching operations, and voltage deviations as loads vary on the network (Pepermans et al., 2005; Dreisen and Katieraei, 2008). In cases where environmental regulations are mandating increased use of clean renewable energy sources such as solar- and wind-generated power, distributed generation delivers power more efficiently when co-located with the load it serves. When distributed generation is combined with storage, controllable and uncontrollable loads, and an active distribution network that enables bidirectional power exchanges with the utility grid, the result is a system architecture that enables very efficient delivery of energy, reliable power supply with differentiation in power service quality, and the ability to operate some or all building systems autonomously off the grid in the event of power outages.

Some electricity end uses in buildings require high power quality and reliability, so real time load management and demand response strategies can be used to mitigate power fluctuations due to intermittent power generation from distributed energy resources or variability in supply from the grid. Cost and environmental impacts are additional factors for consideration; distributed energy sources can be used during peak periods when electricity from the grid is expensive.

Controllable window, shading, and daylighting technologies provide an interesting opportunity to manage end use demands in ways that both complements the peak output profile of solar photovoltaic (PV) electricity generation and counteracts the peak demands on the utility grid produced by daytime commercial activities. In California, for example, air conditioning and lighting loads constitute over 60% of the peak summer commercial building end use load profile (Brown and Koomey, 2003), both of which are heavily influenced by the building facade. Proper design and control of the facade can reduce solar and thermal loads that contribute to peak cooling energy demand in perimeter zones, while daylighting can reduce lighting demand by admitting sun or skylight, enabling lights to be dimmed or shut off when the solar resource is at its peak output. With active façade controls, tradeoffs between solar control and daylight admittance can be optimized to minimize total loads. In the event of complete islanding due to power outages or other reasons, this load management capability can help make off-grid buildings potentially more livable and resilient – which is ultimately synergistic to ambitious zero net energy goals.

Integrating the demand side control with supply side control systems has been investigated in previous studies. Wu and Xia 2015 discuss an approach to achieve optimal switching of supply side resources for demand side management, but demand in this case is defined by time-of-use rate charges and optimal control refers to methods to switch control of a hybrid PV-diesel-battery system to minimize energy cost. Similarly, Hanna et al. 2014 investigated control of supply side resources to minimize time-of-use energy cost and peak demand charges, focusing on optimizing the battery storage dispatch strategy based on solar and load forecasts. Wang et al. 2011 proposed a multi-agent based control framework for integrated demand-supply side control, using simulations to demonstrate how genetic algorithms can be used to determine the optimum setpoints for building equipment (i.e., temperature, illuminance, and CO_2 levels for heating/ cooling, lighting, and ventilation components, respectively) and use of microgrid sources (PV and battery) to balance power consumption and occupant comfort. Here, active control of building loads in coordination with supply side resources fit the definition of demand-supply side control used in this study. Similarly, Stluka et al. 2011 evaluated the technical challenges of achieving optimal demand and supply side control. To implement control, Stluka formulated a solution where the load is disaggregated into a fixed base load and a non-negative controllable load, and the controllable load is assumed to be fragmentable over the time horizon and non-discretionary. A sequential quadratic programming (SQP) solver was then used to find the optimal demand-supply solution for the nonlinear optimization task. The optimization was implemented to control heating and cooling equipment and combined heat and power (CHP) units serving a 850-bed hospital in the Netherlands then operated subsequently for eight years.

This paper examines the synergies between controllable façade technologies and distributed energy resources, namely photovoltaic generation and electricity storage, to determine whether facade technologies can play an enabling role in supporting a desired level of service at either minimum operating cost or minimum carbon footprint. The challenges of coupled demand-supply side control optimizations are described and solved using a two-part approach that is similar conceptually to the method used by Stluka. Performance outcomes of such control are investigated using building energy simulations. A full-scale field test is used to demonstrate feasibility under real weather conditions. Outcomes are used to frame the challenges and benefits of integrating control of dynamic building envelope technologies with the new model of supplying electricity in a liberalized market.

2. Approach to demand-supply control optimizations

The approach used in this study is based on prior work in order to expedite exploration of the technical and market related issues associated with integrated demand-supply side controls. Therefore, the proof-of-concept solution described in this study was not intended to be widely replicable. On the demand side, prior work with model predictive controls for dynamic façade, lighting, and HVAC systems was leveraged (Coffey et al. 2013). On the supply side, the Distributed Energy Resources Customer Adoption Model (DER-CAM), developed by the Lawrence Berkeley National Laboratory (LBNL), was used (Marnay et al., 2012; Stadler et al., 2012). This software is an optimization tool that determines how controllable supply side resources should be operated to minimize the site's total energy bill (electricity and natural gas) or CO_2 emissions, given inputs of the building's end-use energy loads and energy tariff structure and fuel prices. DER-CAM is implemented as a mixed-integer linear model in GAMS (General Algebraic Modeling System).

Dynamic facades technologies, such as electrochromic windows or motorized shading or daylighting technologies, have variable solar-optical and/or thermal properties that can be actively controlled in real time. However, there are complex non-linear physical relationships between the configuration of such shading systems and energy service requirements for cooling, heating, and lighting (not to mention comfort and amenity effects). These interdependencies make dynamic facades hard to include in a global optimization alongside resources such as engine generators or PV arrays, which are readily represented in mixed-integer linear optimization problems by simple fuel cost, heat rate, waste heat production, insolation patterns, etc. On the one hand, creating models that comply with the linearity restrictions required by the mixed integer linear programming of DER-CAM is a major analytic challenge. On the other hand, moving to non-linear optimization poses major runtime and stability barriers.

For this study, a proof-of-concept control system was developed by approximating the non-linear portion of the system as a lookup table, then using the lookup table as a mixed-integer linear system representation within DER-CAM to determine the control state of the demand and supply side components through global optimization of the overall system. The objective function of this study was to minimize the time-of-use electricity bill from the local utility company. Controllable parameters included the switched state of an electrochromic window, charging and discharging of electrical storage, and sale or use of PV power. End user comfort was not included in the objective function. The approach, called DER-CAM_{df} in this study, is outlined below and described in more detail in Gehbauer, 2014.

2.1. Base load

The base load is defined here as the load for a static reference window condition, unmodified by changes produced by the dynamic façade system. Use of pre-calculated loads using typical meteorological year (TMY) data instead of in-situ loads calculations using the actual weather forecast data enables the entire

Table 1. Grid of conditions for dynamic façade

	min	max	step size
Month	6	12	1
Hour	6	18	2
Temperature (°C)	0	30	5
Direct normal solar irradiance (W/m^2)	100	1000	100
Indirect horizontal solar irradiance (W/m^2)	100	900	200

optimization to be completed within about an hour running on a server (i.e., (16) 2.67 GHz quadcore processors). If all of the load calculations, for example, were conducted within DER-CAM, the optimization would take about 50 h.

The base load is determined using the EnergyPlus building energy simulation program where the building geometry and construction, internal loads and schedules (lighting, plug, occupant), and TMY weather data are input to produce a building load database of space conditioning (cooling and heating) and lighting at 5 min intervals over the year. Controllable elements in the building (e.g., shading or daylighting facade components) that are part of the demand-supply side optimization are set to a fixed default position to establish the base load. The HVAC system and central plant are not modeled; cooling and heating energy are calculated using a fixed coefficient of performance (COP) or heating efficiency.

2.2. Dynamic façade lookup table

To determine the load perturbations produced by the demand side controllable elements, separate calculations are made to generate a lookup table of the incremental differences in cooling, heating, and electric energy use resulting from different positions or states of the façade system compared to the loads at the default fixed position. These "offset" values are used with the base load database as inputs to DER-CAM when generating the final control schedule.

Building geometry and construction are input into Radiance and Modelica simulations, then cooling, heating, and electricity loads are generated and stored in a lookup table for a regular grid of outdoor conditions and for each possible state of the dynamic façade device. Conditions include month, hour, outdoor air temperature, direct normal irradiance, and diffuse horizontal irradiance; the grid is defined by minimum and maximum values and a fixed step value (e.g., 0-30°C, 5°C step value, 6 grid points, Table 1).

The three-phase method (*dctimestep*) in Radiance (Ward et al. 2010) is used to determine indoor daylight illuminance levels, absorbed solar radiation on the glazing and shading layers of the façade, and incident solar radiation on room surfaces. The latter two outputs are used as input to the Modelica window (Nouidui et al. 2012) and room thermal models to calculate window heat gains and perimeter zone thermal loads. The model is run for a 15 min simulation period to reach a near steady state (the model assumes light weight construction and a near-constant zone temperature) then the heating or cooling energy requirements are determined. The cooling or heating offset for each discrete state of the device is defined as the difference between the energy use at the default shading position and the new shading position.

Daylight illuminance levels are used to determine the amount of supplementary electric lighting needed to meet the setpoint illuminance level. The electric lighting dimming load profile is then used to determine

lighting energy use. The offset is determined assuming a base lighting load at full power. For a more detailed description of the method for the load calculation, see Coffey et al., 2013.

2.3. Demand/ supply side control schedule

The final control schedule for both demand and supply side components is generated with an N-day forecast horizon as follows (N=7 for purposes of discussion below):

1) Obtain a 7-day weather forecast for outdoor air temperature, sky cover, and global irradiation from a local source (e.g., National Oceanic and Atmospheric Administration (NOAA)). Derive diffuse horizontal and direct normal irradiance from the weather data.

2) For each 15-min time step over the 7-day forecast horizon, determine the base load (cooling and electric load) for the forecast weather condition. The base load is selected from the base load database by first filtering for the month and time step (e.g., 30 data points for the 30 days in March at 12:15 PM), and then identifying the data point where the combined relative error between the forecast and TMY weather data is minimized. Loads are piecewise interpolated by hourly averages of 5 min loads, which are then interpolated to 15 min time steps.

3) For each 15-min time step over the 7-day forecast horizon, find the set of offset values for cooling and electricity use produced by dynamic façade control for the forecast weather condition. The set of offset values (e.g., cooling and electric loads for each of the N possible states of the electrochromic window) are selected from the lookup table by filtering for month, hour, and weather condition. The offset values are not interpolated.

4) Compute the 7-day ahead operation schedule using the weather forecast, electricity tariff schedule, base load and offset values as inputs into the DER-CAM software. For each time step, the software determines the optimal combined states of demand and supply components, taking into account many variables such as the availability of the PV resource, battery state of charge, status of the thermal energy storage, and upcoming electricity rate over the 7-day forecast horizon. Scheduled values are produced for the dynamic façade, thermal energy storage charge or discharge rate, electrical storage charge or discharge rate, use of mechanical cooling versus absorption cooling, use of energy production or sale back to the grid, etc. that best minimizes energy cost or carbon emissions.

3. Simulated performance

3.1. Case 1: Private office in Berkeley, California

3.1.1. Modeling assumptions

A typical private office was modeled to evaluate the energy cost savings produced by a dynamic versus static façade in combination with distributed energy resources in Berkeley, California. The 3.0 m by 4.57 m (13.9 m^2) office was modeled with large-area, south-facing electrochromic windows (6.78 m^2, window-to-wall-area ratio (WWR) of 0.59), an opaque exterior wall with an assembly U-value of 0.20 W/m^2-K, adiabatic thermal coupling of the interior walls, and dimmable light-emitting diode (LED) overhead lighting (12.9 W/m^2, 500 lux setpoint, minimum power of 25%). The lighting was scheduled to be on and daylight responsive between weekday hours of 7 AM to 7 PM local time and off the remainder of the weekday hours and on weekends. Occupancy and equipment loads were not modeled since these were not

emulated in the field test (see Section 4.1). The cooling load was converted directly from the loads using a fixed coefficient of performance (COP) of 3.5, assuming an indoor setpoint temperature of 24±1°C.

Electrochromic (EC) windows have thin, multilayered, solid state coatings on glass that switch from a clear to dark blue tinted state with a small applied voltage (3-5 V direct current (DC)) while maintaining a transparent view to the outdoors. The electrochromic coating has dynamic solar-optical properties that modulate both daylight and solar heat gains through the windows (visible transmittance (Tvis) of 0.01-0.60, solar heat gain coefficient (SHGC) of 0.09-0.41, U-factor of 1.59 W/m^2-°K).

The EC window in the private office was subdivided into three zones (lower, middle, upper) and each zone was controlled to four discrete levels of tint (Tvis=0.01, 0.06, 0.18, 0.60; SHGC=0.09, 0.10, 0.15, 0.41), which resulted in 64 possible control states. The lookup table for the 64 EC window control states was generated at a fine resolution to reduce the error between the TMY and forecast weather conditions. The modeled grid of conditions included 17,150 daytime weather permutations. Power to the window zones to both tint (about 2.7 W/m^2-window) and hold (1.5 W/m^2-window) the windows to a given tint level was not modeled in the simulations. The electrochromic coating switches slowly so tinting lagged the command by 10-30 min, depending on amount of tinting required, incident solar irradiance, and the outdoor air temperature. This delay was also not modeled.

Direct current (DC) power to the EC windows, lighting and HVAC (electric chiller) systems were supplied from a combination of power from the utility grid via bidirectional alternating current (AC) to DC power converter and power from the DC-powered distributed energy resources grid, consisting of a 1.68 m by 1 m, 200 Wp polycrystalline photovoltaic panel (oriented 30° west of due south, tilted 10°, η = 12 %) and a 540 Wh battery. Power losses of approximately 2-3% due to conversion from AC to DC and transmission losses over the DC-powered grid were not modeled.

The electricity time-of-use tariff consisted of energy and demand charges for off-peak periods during the night, mid-peak periods during the day, and on-peak periods with the highest rates between noon and 6:00 PM (Pacific Gas and Electric Company, 2015). PV sales to the utility grid were compensated at a lower rate (Pacific Gas and Electric Company, 2012). See Tables 2-3.

To generate seasonal and annual results, DER-CAM_{df} was run to produce a 15-min operating schedule with a 7-day forecast horizon for each of six representative weeks (weeks 2, 15, 21, 27, 34, and 40; two each for the spring and summer seasons) using TMY data. The number of weeks was constrained by the long run time for the optimizations. The results for each season were multiplied by the number of weeks per season to determine annual performance. DER-CAM reports the total energy cost and CO_2 emissions as well as the total original electric load, dynamic façade offset to the electric load, and sources of electricity used to meet the net load at 15-min intervals. It also reports the battery state of charge (SOC) and sales to the grid from on-site generation.

3.1.2. Summer load profile

Figure 1a shows the electricity load profile for a week in the summer. The total base load (EC window set to the clear state (SHGC=0.41), no DER grid) is shown with the solid black line. Total peak electric loads due to the cooling and lighting systems reach a maximum of 330 W or 23.7 W/m^2 (2.2 W/ft^2; ventilation and heating are not included). The "offset shading" shows the decrement in the total load produced by active DER-CAM_{df} control of the EC window with the objective of minimizing electricity cost. Further decrements to the electric load shape are produced by on-site use of PV generation and battery storage

Table 2. Demand-metered time-of-use utility rates

		May-Oct	Nov-Apr
Rate ($/kWh)	On peak	0.16533	-
	Mid peak	0.11193	0.10485
	Off peak	0.07697	0.08097
Demand ($/kW)	On peak	19.03	-
	Mid peak	4.42	0.24
	Off peak	0	0
	Peak	13.67	13.67
Schedule	On peak	Weekday: 12:00-18:00	-
	Mid peak	Weekday: 8:30-12:00 & 18:00-21:30	Weekday: 8:30-21:30
	Off peak	Weekday: 21:30-8:30; Weekend: 0:00-24:00 (same schedule all year)	

Table 3. Sale price for photovoltaic generation

		Oct-Feb	Mar-May	Jun-Sep
Rate ($/kWh)	On peak	0.0968440	0.1074088	0.2095352
	Mid peak	0.0827576	0.0792360	0.0986048
	Off peak	0.0581064	0.0537044	0.0519436
Schedule*	On peak	Weekday: 12:00-20:00		
	Mid peak	Weekday: 6:00-12:00, 20:00-22:00; Weekend: 6:00-22:00		
	Off peak	Weekday and weekend: 22:00-6:00		

* Same schedule all year.

during the daytime. The utility grid provides the remaining power to meet the load. PV sales to the utility grid are possible on some summer days and on the weekend (days 6-7).

The final electric load shape is shown in Figure 1b. Here, the total base load is again shown as the solid black line and the total cooling load is shown with the red line. The difference between the two lines is the lighting load. A lower electricity demand from the utility grid is the result of the optimization, with almost zero energy consumption during the peak noon hours. As power is drawn down from the fully-charged battery in the early afternoon until sunset, power from the utility increases to meet the remaining load but never increases above a power level of about 60 W (5 W/m^2, 0.47 W/ft^2). This flat plateau produced by optimal control mitigates demand charges. The battery is then charged from the utility grid at night when tariffs are at their lowest rate.

The economics of sizing the PV and storage to the capacity selected for this example plays a factor in the load shape results. The capacity for the PV was sized based on the peak electric load with the dynamic façade being controlled for energy minimization and the practicality of installing the requisite area on the

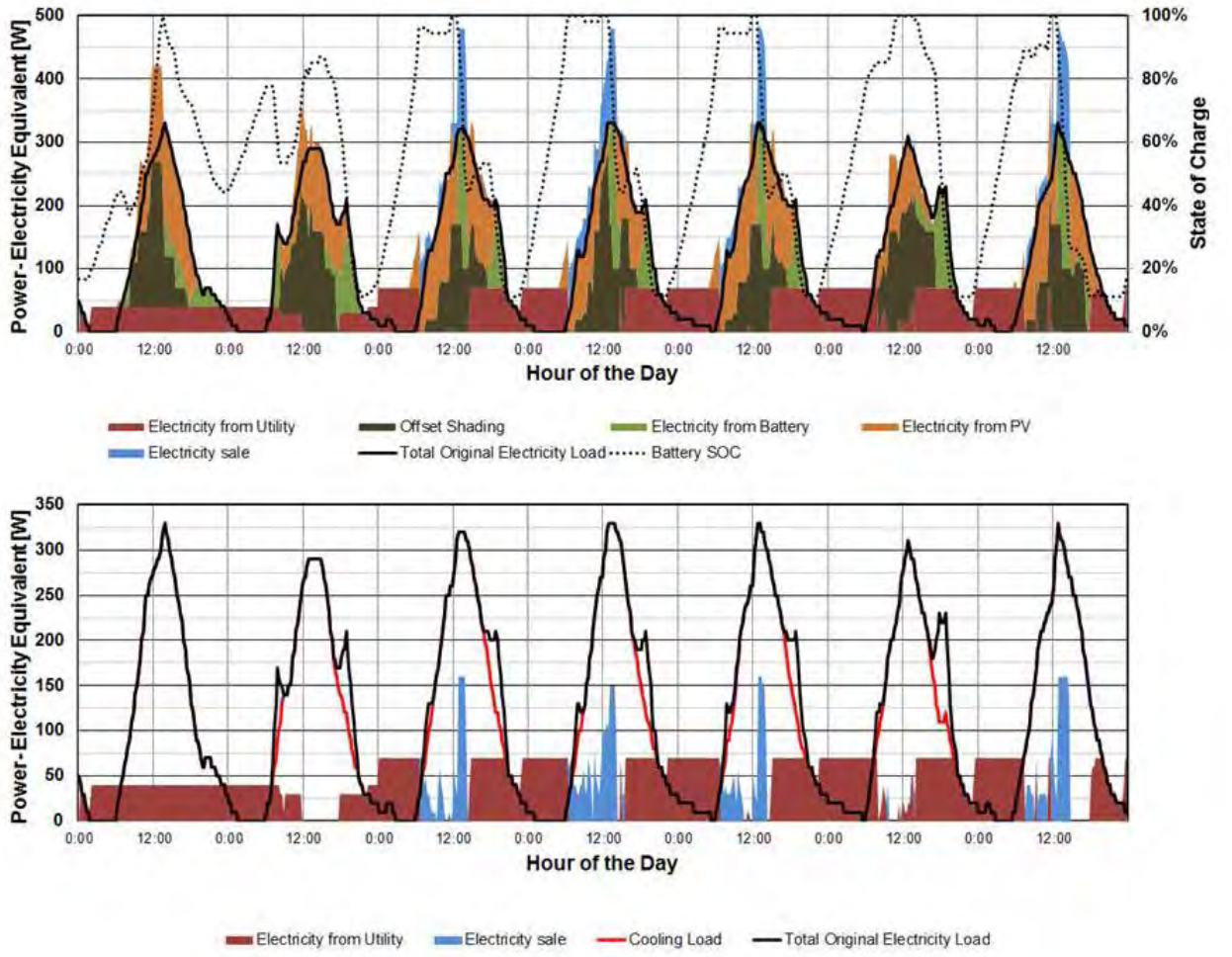

Fig. 1. (a) Above: Simulated summer electricity load profile (W) for a private office zone with a clear static electrochromic window (SHGC=0.41, WWR=0.59) and dimmable LED lighting. The stacked bar indicates how the load is met by DER-CAM$_{df}$ optimal control of the dynamic EC window ("offset shading") and DC distributed energy resource (DER) grid consisting of a 200 Wp photovoltaic panel, 540 Wh battery storage, and the utility grid with an objective of minimizing time-of-use electricity costs. The battery's state of charge (SOC) is given on the second y-axis. (b) Below: Simulated electricity load profile (W) for the same condition as (a) showing utility energy use and PV electrical sales back to the utility. The weekend is the last two right-hand days on the plots. Data are given for a 13.9 m^2 south-facing perimeter office in Berkeley, California.

building or around the site. The electrical storage was sized so that it would be fully discharged over the course of a peak summer day. Lower installed capacity will diminish the impact on the load profile.

3.1.3. Annual energy cost and CO_2 emissions

A comparison is made to quantify the cost benefit of using a dynamic EC window versus a reference static window (EC window in its clear state) with the DER grid. Both the reference and test cases were modeled with the same lighting, HVAC, and DER grid systems. In both cases, DER-CAM$_{df}$ was used to determine the optimal state of the controllable devices to minimize electricity cost. In the reference case, lighting energy use is minimal because the reference window is unshaded, providing a conservative estimate on potential savings. A more realistic case would include operable shades that are lowered to control glare,

which in turn would raise lighting energy use and increase savings due to the dynamic EC test case). This comparison, however, allows us to focus the analysis on the benefit of the dynamic windows within the DER grid context with a clean reference case.

For a typical meteorological year, annual electricity cost savings are \$10.94/m^2-floor-yr (\$1.01/ft^2-yr) or \$22.44/m^2-window-yr (\$2.23/ft^2_w-yr)[2]. Energy costs include demand and energy charges for electricity but not natural gas. Investment cost recovery was not considered in this analysis. Seasonally, the dynamic EC windows provide greatest cost savings during the summer and fall periods because on-peak tariffs are in effect between May and October.

If near net zero energy buildings are defined as buildings that are minimally dependent on energy sources derived from fossil fuels, then this active perimeter façade system in combination with the DER grid is near to accomplishing this goal. Total annual site electricity use from the utility grid (including occupant and equipment loads) is 158 kWh/m^2-yr (50 kBtu/ft^2-yr) for the static window reference case and 132 kWh/m^2-yr (41.9 kBtu/ft^2-yr) for the EC dynamic window test case, or 16% savings. If the PV capacity was resized to the maximized case defined by Griffith et al., 2007 (i.e., 65 kWh/m^2-yr annual PV production) then the total annual site electricity use would be 20.3 kWh/m^2-yr (6.4 kBtu/ft^2-yr). Griffith et al. estimated a maximum technology energy efficiency scenario with PV of 38 kWh/m^2-yr (12.2 kBtu/ft^2-yr).

Note that the total energy expended to meet the load, when supplied by a mixture of utility and DER sources, is greater than the utility energy use alone due to the losses associated with charging and discharging the battery. In this modeled scenario, the objective was to minimize energy cost as reflected by the time-of-use rates. If the tariff schedule is marginally related to environmental impacts (where peak energy is supplied by fossil fuel-based power plants), then the balance of using fossil fuels versus clean energy is reflected economically in part in the utility cost savings. Investment calculations should include utility cost savings as well as environmental and resiliency benefits. Also note that tariffs will change over time.

California's carbon dioxide emissions per unit of electricity produced is on average 0.44 kg_{CO2}/kWh and ranges from zero to double the average over the year (E3, 2010). Annual CO_2 emission savings due to the dynamic EC window test case were 15.0 kg_{CO2}/m^2-yr (1.39 kg_{CO2}/ft^2-yr) compared to the reference case, both using the cost minimization mode. If the DER-CAM_{df} optimization objective is set to minimize CO_2 emissions, then total annual utility electricity cost increases but annual CO_2 emission savings raises to 16.5 kg_{CO2}/m^2-yr (1.53 kg_{CO2}/ft^2-yr). This added CO_2 emission savings comes at an energy cost of \$ 0.033/m^2-kg_{CO2}-yr (\$0.003/ft^2- kg_{CO2}-yr).

Part of these costs could be defrayed on the spot market. The price for a certified savings for one kilogram of CO_2 emissions on the European Emissions Allowances (EUA) Auction is \$0.0086/kg_{CO2} (EEX, 2014). At this low price, however, the commensurate rise in energy cost of \$0.68/m^2-yr (\$0.063/ft^2-yr) with CO_2 minimization controls could be defrayed by \$0.00092/m^2-yr (\$0.000086/ft^2-yr).

.

[2] Unless otherwise noted, data per m^2 or per ft^2 are given in per floor area. Data per m^2 or ft^2 of window area will be denoted by m^2_w or ft^2_w.

4. Measured performance

4.1. Field test set-up

A field test was conducted at the Advanced Windows Testbed, Berkeley, California to evaluate the feasibility of implementing integrated control of demand and supply side resources and to measure the performance of the system under real sun and sky conditions. The testbed consists of three identical, side-by-side private offices facing due south and is fully instrumented so that lighting and HVAC energy use, control operations, source energy, and comfort can be measured (Fig. 2). Each of the test rooms are thermally isolated using a conditioned guard space between test rooms, ceiling and roof so that near-isothermal conditions surround each test cell, enabling simultaneous comparative measurements of heating and cooling energy between test rooms. A detailed description of the facility in general is given in Lee et al., 2006.

Two reference rooms were set up: (a) one with a conventional low-emittance window (Tvis=0.62, SHGC=0.40, U-value=1.7 W/m^2-°K) with an indoor matte-white fully lowered Venetian blind with its slat angle set to just block direct sun ("Reference-VB"), and (b) the second room with a three-zone electrochromic window (same as the simulated case in Section 3) switched in response to outdoor photometric sensor inputs using a heuristic control algorithm provided by the manufacturer ("EC-heuristic"). Both rooms were fitted out with daylight-responsive, dimmable LED lighting (6.1 W/m^2 installed load, 300 lux setpoint, minimum power of 25%). All loads were powered with conventional AC from the utility grid.

The third test room was set up with the same three-zone electrochromic window and lighting systems as the reference room (b) but with a DC DER grid ("EC-DER-grid"). The DER grid supplied DC power to the lighting$_{DC}$ and HVAC$_{DC}$ systems from a south oriented 270 Wp PV panel (1.68 m^2, η = 16.1 %), 540 Wh lead acid battery, and the utility grid. The DC powered lighting avoided transformation losses of about 5%, decreased power consumption to 6.5 W/m^2 at 300 lux and enabled a minimum power level of 0%.

The operational schedule for the EC window zones and PV, battery, and utility grid power use was calculated using DER-CAM$_{df}$ with a 24-h forecast horizon at midnight, then recalculated with the same forecast horizon each time the NOAA weather forecast was updated (i.e., 3 AM, 2 PM, 10 PM). Scheduled values were sent at 15-min intervals via HTTP using an IP-enabled microcontroller (Raspberry Pi) to the testbed central server, which passed the commands to a LabView National Instruments interface to control the actual devices.

Lighting and plug loads were measured directly. Plug loads were those that supported instrumentation in the test rooms and were not designed to emulate equipment loads in a typical commercial office building. Typical occupant loads were also not emulated since the analysis was focused on demonstrating the between-room difference in performance due to the envelope and lighting systems. The window area was the same between the three test rooms (6.78 m^2). The opaque window wall envelope loads in the three test rooms were minimized using polyisocyanurate foam boards within the curtainwall system; the assembly U-value was approximately 0.20 W/m^2-K.

HVAC loads were calculated by determining the net thermal load due to the window and lighting system then converted to electricity use using a COP of 3.5. The net thermal load was determined by measuring the HVAC system load needed to maintain a constant setpoint temperature of 24±1°C (electric resistance heater, chilled water supply flow rate and inlet and outlet temperatures, fan) then subtracting thermal loads that were non-comparable (plug loads) between the three test rooms as described in Lee et al. 2006. The

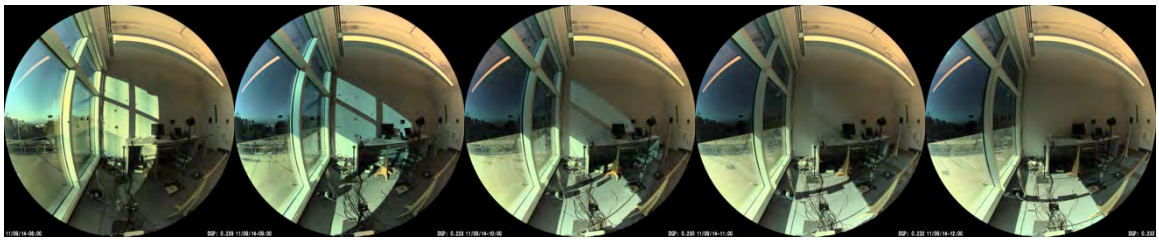

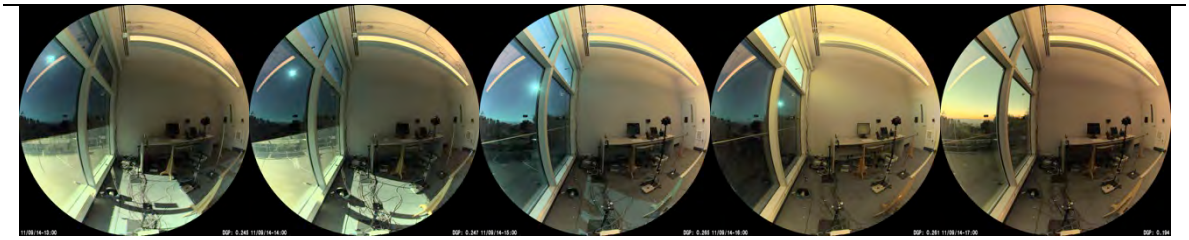

Fig. 2. (a) Above: Outdoor photograph of the Lawrence Berkeley National Laboratory Advanced Windows Testbed in Berkeley, California with electrochromic windows installed in the lefthand and center test rooms and low-emittance windows with a Venetian blind (currently raised) in the righthand test room. (b) Below: Indoor photographs of the three-zone electrochromic window being switched over the course of a sunny day with heuristic controls on November 9, 2014.

HVAC electrical use was implemented as a false load on the DC DER grid using variable electrical resistors in order to properly demonstrate feasibility of the integrated control system. Source electricity use and production for the DER grid were also measured directly.

Table 4. Suggested definition of daylight glare comfort classes (Wienold 2009)

Max DGP of 95% of period		Avg DGP of 5% of period	Class	Meaning
≤ 0.35 imperceptible		≤ 0.38 perceptible	A	Best
		> 0.38	B	Good
≤ 0.40 perceptible		≤ 0.42 disturbing	B	Good
	and	> 0.42	C	Reasonable
≤ 0.45 disturbing		≤ 0.53 intolerable	C	Reasonable
		> 0.53	Discomfort	Discomfort
> 0.45 disturbing		> 0.53	Discomfort	Discomfort

With multivariable control, many of the perimeter zone and system design parameters needed for the analytical models are unknown and costly to determine. To reduce forecast error during real-time operations, the base load and shading offset models were calibrated daily using measured data from the previous day. Several adjustments were also made to better emulate the real-time conditions of the systems. The switching speed of the electrochromic is dependent on environmental conditions. For field testing during cool winter conditions, the electrochromic's slow switching response time was compensated for by sending the commands to the EC controller one time step (15 min) earlier. The field test showed a 30-min phase shift between the monitored and forecasted thermal load. To emulate this effect of thermal mass, the forecasted building load was shifted 30 min ahead to improve performance.

For analysis, the actual weather conditions were recorded on site (i.e., direct normal irradiance, global horizontal irradiance, outdoor air temperature). Although not addressed explicitly in the control algorithm for the EC-DER-grid test case, visual comfort was assessed using time-lapsed high dynamic range (HDR) imaging every 5 min. Measurements were taken in the center of the room looking toward the window at a distance of 1.5 m from the window and parallel to the window at a distance of 0.91 m from the window, both at a height of 1.22 m above the floor. The HDR images were post-processed to determine the daylight glare probability (DGP) index for each time step for the period of 8:00-18:00. The data were then rank ordered to determine the maximum DGP value of the lower 95% of the data for the period of evaluation and the average DGP of the upper 5% of the data. These two values determine the class of glare discomfort as defined in Table 4 (Wienold 2009).

4.2. Results

In Figure 3a, the total electric load due to cooling and lighting for the EC-DER-grid test case is shown as a solid black line and then the decrements in electricity use due to the DER sources are shown as infill colors below and above this line. In the early morning, the total load shows the lights turned on then dimmed when there is adequate daylight, then as the day progresses, the load increases to a peak in the early afternoon reflecting the increased cooling load due to solar heat gains. For the four days in the latter half of the period, the PV and battery supply the majority of the power during the daytime then the utility power peaks in the late evening when the battery is recharged (the battery's state of charge on the graph shows erroneous dips due to the way the current is measured). For the preceding two days, however, there is considerable use of utility power in the early morning to about mid-day due to significant discrepancies between the forecast and actual weather data. Figure 4 shows the forecast and actual weather data for the week. The weather forecast under-predicted peak solar irradiance levels by 500 W/m^2 and outdoor temperatures by 4°C, causing the forecasted total load to be lower than actual and thus requiring daytime

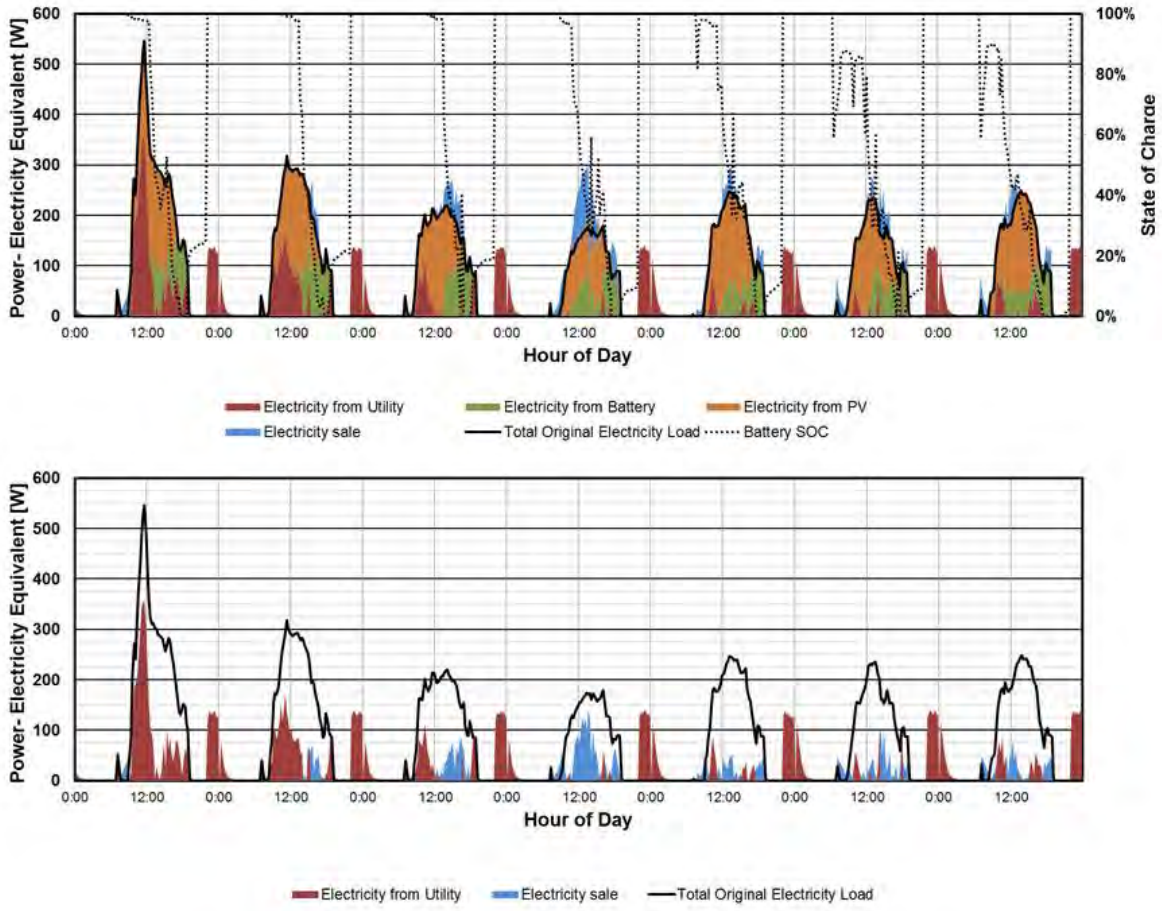

Fig. 3. (a) Above: Monitored winter electricity load profile (W) for a private office zone with a dynamic electrochromic window (SHGC=0.09-0.41, WWR=0.59) and dimmable LED lighting. The stacked bar indicates how the load is met by DER-CAM$_{df}$ optimal control of the DC DER grid consisting of a 270 Wp photovoltaic panel, 540 Wh battery storage, and the utility grid with an objective of minimizing time-of-use electricity cost. The battery's estimated state of charge is given on the second y-axis. (b) Below: Monitored electricity load profile (W) for the same condition as (a) showing utility energy use and PV electrical sales back to the utility. Data are given for a 13.9 m^2 south-facing perimeter office in Berkeley, California for February 20-26, 2015.

use of utility power to satisfy the load. (Note that this discrepancy did not occur in Section 3.1 because the forecast and actual weather data were the same for the simulated energy analysis.)

A comparison of the utility grid load profiles for the three rooms is given in Figure 5. The reference room with an indoor Venetian blind and the test room with heuristically controlled EC windows exhibit the typical bell-shaped load profile with the peak in the mid-afternoon. With optimized control of the DER grid and EC window, the utility loads due to the window and lighting system are flattened considerably; daytime peak demand is reduced to about 70 W (5 W/m^2) in the latter half of the week. Utility grid cost was calculated using the same PG&E E-19 and E-SRG tariffs from Section 3.1. The monthly demand charge, which is set by the highest peak in each accounting period, was divided equally amongst the days. The resultant electricity cost for the whole week was $3.19 for the reference room with Venetian blinds, $2.17 for the heuristic-controlled EC windows, and $1.61 for the integrated EC-DER-grid test room, or a savings of 32% and 50% relative to the reference room, respectively. If the first three days are ignored, then savings for the integrated EC-DER-grid room would be 74%.

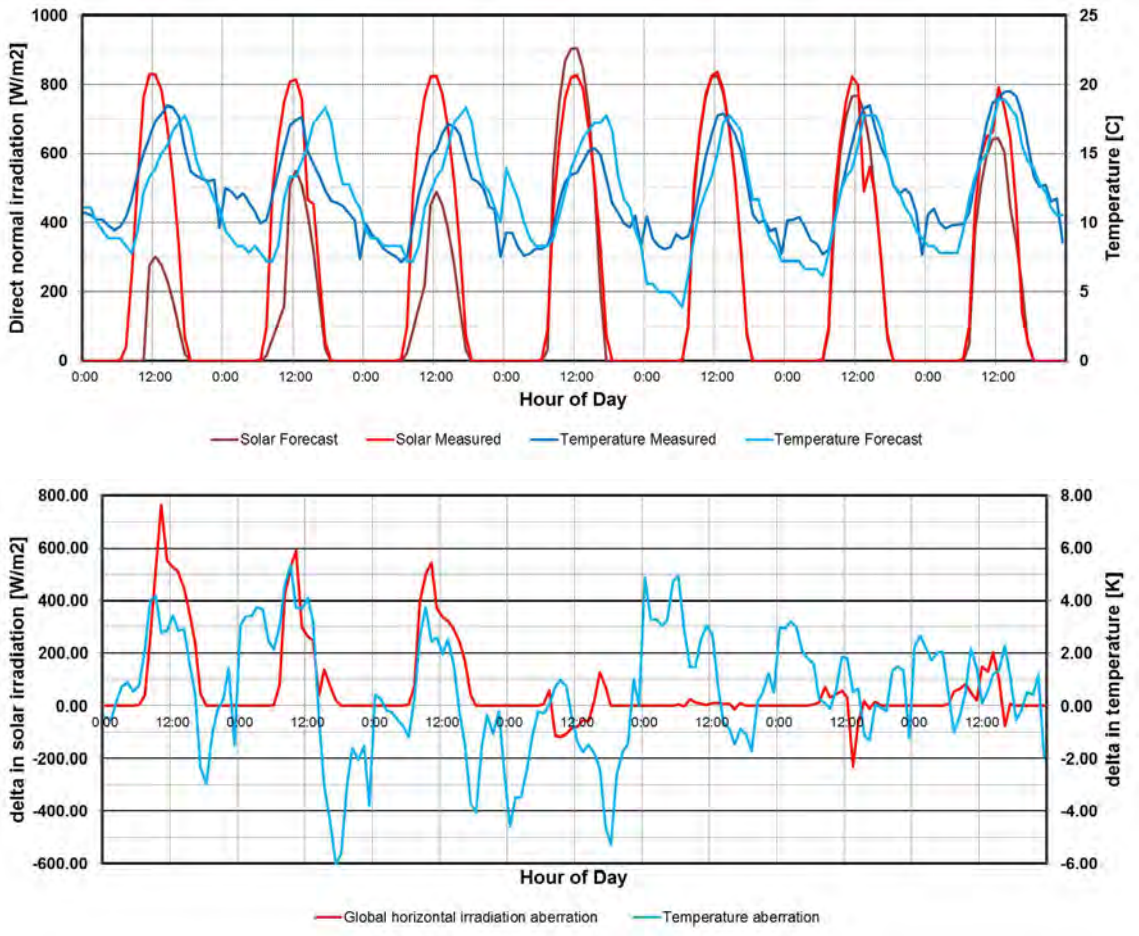

Fig. 4. (a) Above: Forecasted and monitored direct normal irradiation (W/m^2) and outdoor air temperature (°C) for the winter period, February 20-26, 2015. (b) Below: Difference in monitored and forecasted weather data.

An evaluation of the visual comfort resulting from the different modes of control shows trends that are indicative of the problems one can have if comfort is not explicitly accommodated in the optimization scheme (Figure 6). The visual comfort conditions in the integrated EC-DER-grid test room (Room B) were at the "discomfort" (worst) or Class C level (reasonable) over the same example week given in Figure 3. In the case of the heuristically controlled EC windows (Room C) which the vendor indicated was explicitly designed to control glare, the conditions were Class A (best) for the window-facing view for the week, but were "discomfort" or Class C for the view parallel to the window due to late afternoon direct sun (see Figure 2). The reference room A with the static blind shows that the tilt angle was insufficient to control glare. Closing the blind more or tinting the EC glass more would reduce glare to within acceptable levels (DGP<0.35) but increase lighting loads. The degree of this effect will depend on the actual view position of the occupant. The view locations for this assessment were close to the window and therefore fairly conservative.

5. Discussion

The simulations and field test demonstrate how dynamic façade technologies can play an enabling role in combination with distributed energy resources to achieve near zero net energy goals and a desired level of

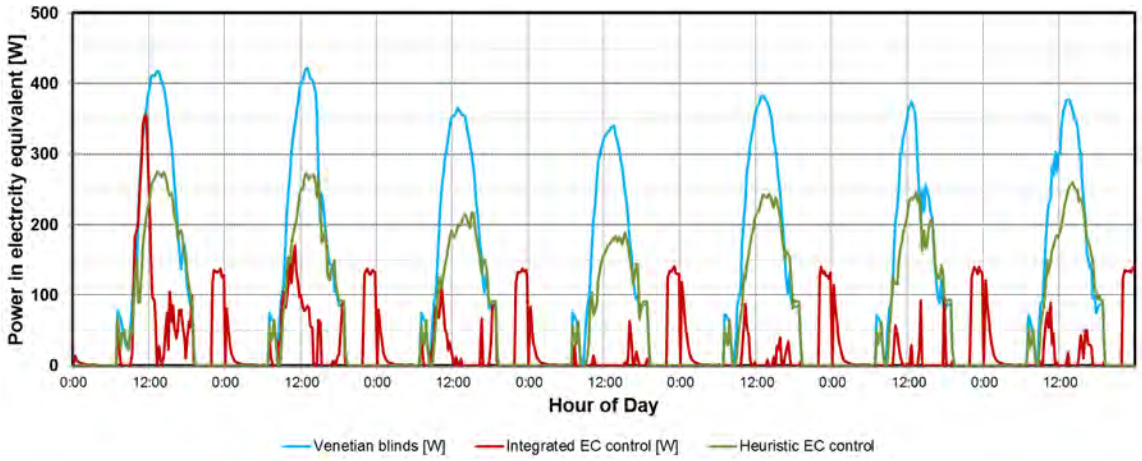

Fig. 5. Monitored winter electricity load profile (W) for a private office zone with (a) a low-emittance window and static Venetian blinds with no DER grid, (b) a dynamic electrochromic window (SHGC=0.09-0.41, WWR=0.59) with heuristic controls and no DER grid, and (c) an integrated system, where the electricity load is met by DER-CAM$_{df}$ optimal control of the electrochromic window and DC DER grid consisting of a 270 Wp photovoltaic panel, 540 Wh battery storage, and the utility grid with an objective of minimizing time-of-use electricity cost. Data are given for a 13.9 m^2 south-facing perimeter office in Berkeley, California for February 20-26, 2015.

electrical service at minimum operating cost. The cost-benefit of doing so will be dependent on many factors, including the cost of the dynamic façade and DER technologies, climate, availability of solar resources at the site, utility grid time-of-use rate schedule, etc. These solutions will be most applicable in areas where the cost of electricity during peak periods more closely reflects fossil fuel's environmental impacts on climate change and the economic impacts on business operations when power services are disrupted.

For the cases where the value proposition is compelling, several practical issues will need to be resolved to scale up these integrated control systems for widespread adoption. ("Scaling" is defined here as control solutions that can "scale" from a single zone to a whole building with hundreds of zones. Conventional, component-oriented heuristic algorithms typically work at a single zone level. For integrated solutions that optimize performance at the whole building and grid level, scalability to many zones is a relevant and challenging design parameter.) This exploratory proof-of-concept study used a combination of existing tools to reduce the complex non-linear physical impacts of demand side control to a simple look-up table that could then be coupled with a mixed integer linear optimization tool to achieve integrated demand-supply side control. This approach solved major runtime and stability barriers and demonstrated feasibility, both of which are necessary steps for achieving practical scaling.

One critical issue is use of a proper and consistent modeling approach that (a) avoids discontinuities that can cause optimizations to fail, and (b) allows re-initialization of all state variables at each time step in order to realign the prediction model with the current temperatures and energy storage levels of the building. Sole use of EnergyPlus, for example, to solve this control optimization problem would be problematic. EnergyPlus was developed for simulation, not for real-time optimization, so heating, cooling, and electrical energy can have discontinuous jumps, for example, if room temperature set points are changed. The solver was implemented in a way that does not constrain the numerical error of the approximations to the state variables. The solver tolerances are coarse to meet the runtime demands of design calculations so optimization algorithms that require smoothness can fail far from the optimum solution (Wetter and Wright, 2004). EnergyPlus also does not allow for state reinitialization within each

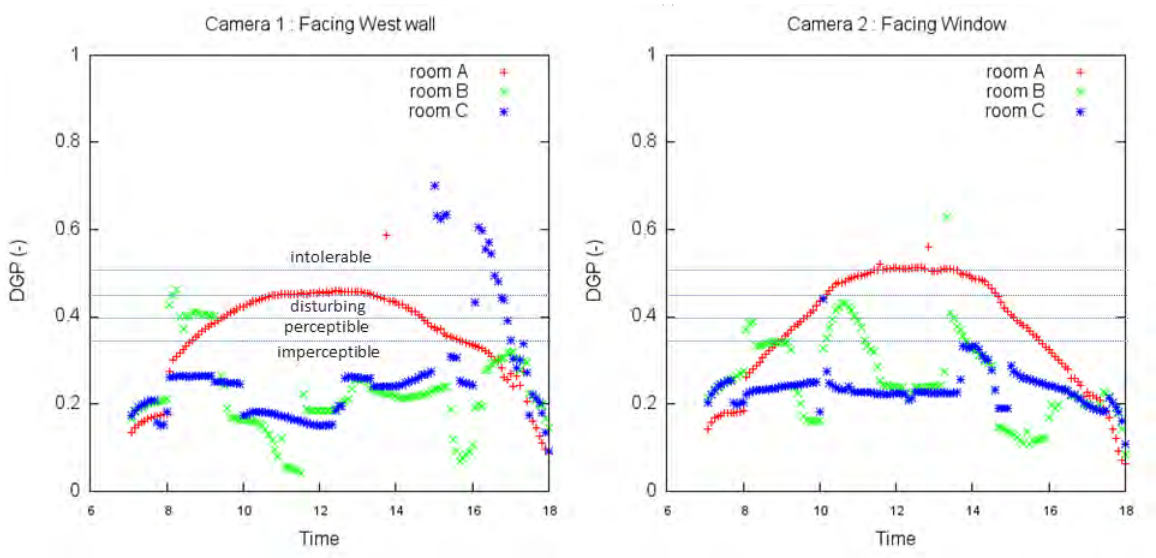

Fig. 6. Example of monitored daylight glare probability (DGP) for a view looking parallel to the window, facing the west wall (left) and looking directly at the window (right). Values are given for Room A with a low-emittance window and static Venetian blinds, Room B with the electrochromic window and integrated EC-DER-grid controls, and Room C with the electrochromic window and heuristic controls. Daily DGP class was "discomfort" for Room A, Class C for Room B, and "discomfort" and Class A for the view facing the west wall and facing the window, respectively, for Room C. Data are given for a 13.9 m^2 south-facing perimeter office in Berkeley, California for February 24, 2015.

time step, so the effects of thermal mass cannot be accurately modeled. On the other hand, Modelica, for example, was developed explicitly for real-time control and solves the above two modeling issues, enabling recalculation of the room heat balance within the same time step and allowing for numerical convergence to within a specified level of error. This tool could be used to solve a coupled demand-supply side optimization problem.

A second critical issue is solving the optimization problem accurately within runtime constraints over the life of the installation. When field testing the proof-of-concept controller, several sources of error were identified that can cause deviations between predicted and measured outcomes: e.g., forecast differs from actual weather conditions, constraints on device actuation or response are inadequately accounted for (e.g., temperature-dependent switching speed of electrochromic windows, durability constraints for motorized shades), or actual building construction and operations that are either unknown or are later modified to suit changes in space use over the life cycle of the building, etc. Whether the initial models are full building physics models, reduced-order models, or black box models, the models will need to be designed to maintain accuracy over the life of the installation using a combination of basic physics, sensor data, or adaptive self-learning model corrections. This will correct for the unavoidable mismatch between the model and actual room, for example, if the space is reconfigured. Model corrections can be made using trended historical data, necessitating a means to archive data from the multiple controlled systems. Computing requirements will need to be reliable and robust if optimizations are to be updated more frequently.

The proof-of-concept field test implementation was run open loop with inputs from the weather forecast. Closed-loop control that uses feedback from sensors and the controlled devices would improve accuracy and performance reliability. This third critical issue is particularly relevant to façade control systems considering their effect on occupant comfort and indoor environmental quality, both of which were not

explicitly addressed in this preliminary approach with negative consequences in the final analysis. Since weather forecasts are fairly inaccurate, a forecasted overcast sky condition that turned out to be sunny could result in significant occupant discomfort and rejection of the control system. Closed-loop control within constraints defined by the supervisory optimal demand-supply side control system would improve performance and end user acceptance of the controls.

The fourth critical issue has to do with the need for real-time coupling between demand side and supply side controls. This issue is unique to façade systems because they influence both lighting electricity use and space conditioning/ thermal energy use. If the "cost" for thermal energy differs from electricity use on the supply side, then the control optimization problem is coupled. If the cost is the same, then the demand side can be optimized independently from the supply side. In the field study described in Section 4, electricity for cooling and lighting energy use came from the same source so control of the EC windows would be the same as an energy-efficiency, demand side management mode of control. When distributed energy resources include thermal energy generation such as combined heat and power (CHP), asynchronous pricing of electricity and thermal energy complicates optimal control. Predictive strategies involving active management of building facade loads in concert with thermal mass storage strategies, for example, can reduce and shift peak cooling loads toward off-peak periods. Low cost or free cooling can be provided by the economizer, natural ventilation, thermal storage due to night time flush strategies, solar thermal to power an absorption chiller – all of which can cause the energy cost ratio between cooling and lighting to vary temporally. For these situations, demand-supply side optimizations are likely to be coupled. For periods when cooling is cheaper than lighting energy use, for example, the dynamic façade might be controlled to open up to admit daylight and reduce lighting energy use, rather than close down to reduce solar loads and cooling energy use. The implication of coupled control is increased complexity and cost at a building wide scale, particularly if the optimization involves an array of heterogeneous zones. For accurate, reliable control, the building control systems would need to be able to communicate or be interoperable with the DER grid. Further investigation is warranted.

The building industry is risk averse and reluctant to adopt automated control systems because of the perceived high cost and complexity of the systems. The more complicated and opaque the control, the less likely the facility management team will be able to troubleshoot or tune the system as complaints arise from occupants or as changes are made to the building. Technological solutions that provide fault detection and diagnostics and tools for monitoring, evaluating, and visualizing performance will be imperative for widespread adoption.

On the subject of hardware infrastructure, motorized shading, electrochromic windows, and LED lighting systems could run natively on DC power to eliminate power conversion losses (the DC DER grid used in the field study above was implemented to investigate technical issues related to DC-powered systems in a separate parallel study). Building integrated photovoltaic power could be supplied at the point of use on a floor-by-floor basis, using a DC-powered, T-bar drop ceiling system for the overhead electric lighting system and direct supply to the dynamic shading and convector unit at the window wall. Electrochromic windows operate on 3-5 VDC and are switched using current-voltage modulators to preserve the durability of the switchable device. However, DER grids are typically powered by AC, where power supplied by the photovoltaic and battery systems is converted to AC using a bidirectional rectifier/ inverter. Use of electric vehicles for electrical storage would be appropriate for this commercial building application if charging was scheduled to occur at night (e.g., campus vehicles).

6. Conclusions

A proof-of-concept simulation and field study was conducted to investigate the upside potential of integrating dynamic façade technologies with distributed energy resources. Integrated control was achieved by coupling pre-existing modeling tools to generate an optimized schedule for controlling the dynamic façade, charging and discharging electric storage, and use or sale of electricity produced by a solar photovoltaic generation system. These tools were used to estimate the annual cost, carbon emissions, and energy use savings for a south-facing perimeter office zone in Berkeley, California given time-of-use rates that charge higher rates during daytime periods of high electric demand. The tools were also used to operate switchable electrochromic windows and a DC DER grid in a full-scale testbed facility at the Lawrence Berkeley National Laboratory so that real-time performance could be measured and verified.

The simulated and measured cases demonstrated that controllable window and daylighting technologies are effective in managing perimeter zone electricity use demand that both complements the peak output profile of solar photovoltaic electricity generation and counteracts the peak electricity demands on the utility grid produced by daytime commercial activities. If the photovoltaic generation is sized to meet the peak load and the electrical storage is sized to be discharged over the course of the peak day, the remaining electric load is a fraction (20%) of the original peak load. The solution enables one to attain near zero net energy goals and produces a more livable daylit environment with controlled cooling loads in the event of a power outage.

The field test demonstrated that such control is feasible but will require further engineering to achieve a robust, replicable solution. Performance objectives were not met consistently due primarily to discrepancies between the forecasted and actual weather conditions. Comfort was also not explicitly addressed. A technical approach for achieving reliable, accurate control was discussed but additional work is needed before such systems can be broadly deployed in the market.

Because facades can impact 30 percent or more of the peak cooling and lighting loads in commercial buildings, dynamic facades as a controllable load can support power quality and reliability (PQ&R) end goals. In the United States, the economics of achieving PQ&R given the utility's aging infrastructure and increased use of intermittent renewable generation source is strong motivation to invest in distributed energy resources. The challenge of promoting use of microgrids to enable islanding or off-grid resiliency however is the investment cost for storage and renewables. Making buildings livable and more comfortable without power is synonymous with zero net energy buildings and controlling peak loads is an integral part of the solution. Dynamic façade technologies such as motorized shading and electrochromic windows are synergistic with these end goals.

Acknowledgments

We would like to acknowledge the contributions of our LBNL colleagues: Michael Wetter, Dennis DiBartolomeo, Darryl Dickerhoff, Wei Feng, and Anothai Thanachareonkit. We would also like to thank Sage Electrochromics and Saint-Gobain North America for their in-kind support for the field test.

Implementation and testing of the loads-to-DERCAM control module was conducted as part of Christoph Gehbauer's master's thesis under the supervision of Professor Hubert Fechner at the Renewable Urban Energy Systems Department of the University of Applied Sciences Technikum, Wien, and financially supported by the Austrian Marshall Plan Foundation.

This work was supported by the Assistant Secretary for Energy Efficiency and Renewable Energy, Office of Building Technology, State and Community Programs, Office of Building Research and Standards of the United States Department of Energy under Contract No. DE-AC02-05CH11231 and by the California Energy Commission through its Public Interest Energy Research (PIER) Program on behalf of the citizens of California.

References

Brown, R., Koomey, J., 2003. Electricity use in California: Past trends and present usage patterns. Energy Policy 31(9), 849-864.

Coffey, B., McNeil, A., Nouidui, T., Lee, E.S., 2013. Automated production of optimization-based control logics for dynamic façade systems, with experimental application to two-zone external venetian blinds. California Energy Commission PIER Technical Report.

Dreisen, J., Katieraei, F., 2008. Design for distributed energy resources. IEEE Power and Energy Magazine, May/ June 2008, 30-39.

EEX, 2014. European Emission Allowances Auction (EUA) | Global Environmental Exchange, Primary Market Auction, www.eex.com, accessed March 8, 2015.

E3, 2010. Energy+Environmental Economics, GHG Tool for Buildings in California, December 2010, v.3, https://ethree.com/public_projects/ghg.php, accessed March 8, 2015.

Gehbauer, C., 2014. A linear optimization framework to operate shading technologies. Thesis, Master of Science in Engineering, University of Applied Sciences, Technikum Wien.

Griffith, B., Long, N., Torcellini, P., Judkoff, R., Crawley, D., Ryan, J., 2007. Assessment of the technical potential for achieving net zero-energy buildings in the commercial sector. Technical Report National Renewable Energy Laboratory, TP-550-41957, December.

Hanna, R., Kleissl, J., Nottrott, A., Ferry, M., 2014. Energy dispatch schedule optimization for demand charge reduction using a photovoltaic-battery storage system with solar forecasting. Solar Energy 103, 269–287.

Lee, E.S., DiBartolomeo, D.L., Klems, J.H., Yazdanian, M., Selkowitz, S.E., 2006. Monitored energy performance of electrochromic windows controlled for daylight and visual comfort. Proc ASHRAE Annual Meeting, Quebec City, Canada, 112(2).

Marnay, C., Stadler, M., Siddiqui, A., DeForest, N., Donadee, J., Bhattacharya, P., Lai, J., 2012. Applications of optimal building energy system selection and operation. Proc IMechE Part A: J Power and Energy 227(1), 82-93.

Nouidui, T.S., Wetter, M., Zuo, W., 2012. Validation of the window model of the Modelica buildings library. Proc SimBuild 2012 Conference, Madison, Wisconsin.

Pacific Gas and Electric Company, 2015. Electric Schedule E-19 Medium General Demand-metered TOU Service, January 2015, http://www.pge.com/tariffs/tm2/pdf/ELEC_SCHEDS_E-19.pdf, accessed March 8, 2015.

Pacific Gas and Electric Company, 2012. Electric Schedule E-SRG, Small Renewable Generator PPA, November 2012, http://www.pge.com/tariffs/tm2/pdf/ELEC_SCHEDS_E-SRG.pdf, accessed March 8, 2015.

Pepermans, G., Driesen, J., Haeseldonckx, D., Belmans, R., D'haeseleer, W., 2005. Distributed generation: definition, benefits and issues. Energy Policy 33, 787-798.

Stadler, M., Cardoso, G., Bozchalui, M.C., Sharma, R., Marnay, C., Siddiqui, A., Groissböck, M., 2012. Microgrid modeling using the stochastic Distributed Energy Resources Customer Adoption Model (DER-CAM). Proceedings of the INFORMS Annual Meeting 2012, Phoenix, Arizona.

Stluka, P., Godbole, D., Samad, T., 2011. Energy Management for Buildings and Microgrids. Proc 2011 50th IEEE Conference on Decision and Control and European Control Conference (CDC-ECC), Orlando, FL, 5150-5157.

Wang, Z., Yang, R., Wang, L., 2011. Intelligent Multi-agent Control for Integrated Building and Micro-grid Systems. Proc Innovative Smart Grid Technologies (ISGT), 2011 IEEE PES Conference.

Ward, G., Mistrick, R., Lee, E.S., McNeil, A., Jonsson, J., 2010. Simulating the daylight performance of complex fenestration systems using bidirectional scattering distribution functions within Radiance. Leukos, Journal of the Illuminating Engineering Society of North America 7(4), 2010.

Wetter, M., Wright, J.A., 2004. A comparison of deterministic and probabilistic optimization algorithms for nonsmooth simulation-based optimization. Building and Environment 39(8), 989-999.

Wienold, J., 2009. Dynamic daylight glare evaluation. Proc Building Simulation 2009, 11th International IBPSA Conference, Glasgow, Scotland, July 27-30, 2009.

Wu, A., Xia, X., 2015. Optimal switching renewable energy system for demand side management. Solar Energy 114, 278–288.